POLITECNICO DI TORINO

Collegio di Ingegneria Chimica e dei Materiali

Corso di Laurea Magistrale
INGEGNERIA DEI MATERIALI PER L'INDUSTRIA 4.0

Tesi di Laurea Magistrale

Analysis of Abrasive Wear of Epoxy-Polyester Hybrid Coatings Functionalized with Hydrotalcites Using Raman Spectroscopy

Relatori

prof. Marco Sangermano
prof. Francisco Javier Velasco Lopez
dott.essa María Fernández Álvarez

Candidato

Luca Gilli

Marzo 2026

Acknowledgements

I would like to thank in particular my tutors Francisco and Maria for helping me develop this project and for showing unwavering patience.

A thank you also goes to Nataly for following me throughout the process, to Carlos III for allowing me to live this fantastic exchange experience and to my classmates for helping me from day one, breaking down any language barrier.

Finally, thank you to the entire research team at the Spanish Institute of Ceramics and Glass, who followed and helped me throughout the development of the thesis.

Abstract

The structure of epoxy-polyester-based coatings is characterized by high chemical resistance, good adhesion, thermal stability, and good mechanical properties.

This Master Thesis is based on the addition of different percentages of hydrotalcite (1% and 3%) into the epoxy-polyester powder coatings, seeking an improvement in the properties of the coating, particularly regarding mechanical properties.

The primary objective is to determine whether the differences between a commercial coating and those obtained with the addition of hydrotalcite can be characterized by Raman spectroscopy. In particular, whether Raman spectroscopy reveals differences in terms of wear between the coatings obtained with or without hydrotalcite.

In order to obtain these results, a homogeneous distribution of the reinforcement in the polymer coating was achieved by means of a phase resonator, applied to steel sheets using an electrostatic gun, and finally, crosslinking was carried out in a laboratory oven.

The coating was characterized by confocal Raman spectroscopy and differential scanning calorimetry; subsequently, properties such as hardness, roughness, and mechanical wear properties were studied. In this study, a more resistant coating was obtained.

Keywords:

Epoxy-polyester, powder coating, hydrotalcite, wear resistance, Raman.

Resumen

La estructura de los recubrimientos a base de epoxi-poliéster se caracteriza por su alta resistencia química, buena adherencia, estabilidad térmica y buenas propiedades mecánicas.

Esta Tesis de Master se basa en la adición de diferentes porcentajes de hidrotalcita (1% y 3%) en los recubrimientos en polvo epoxi-poliéster, buscando una mejora en las propiedades del recubrimiento, particularmente en lo que se refiere a las propiedades mecánicas.

El objetivo principal es determinar si las diferencias entre un recubrimiento comercial y los obtenidos con la adición de hidrotalcita se pueden caracterizar mediante espectroscopia Raman. En particular, si la espectroscopia Raman revela diferencias en términos de desgaste entre los recubrimientos obtenidos con o sin hidrotalcita.

Para obtener estos resultados, se consiguió una distribución homogénea del refuerzo en el recubrimiento polimérico mediante un resonador de fase, se aplicó a láminas de acero utilizando una pistola electrostática y, por último, se llevó a cabo la reticulación en un horno de laboratorio.

El recubrimiento se caracterizó mediante espectroscopia Raman confocal y calorimetría diferencial de barrido; posteriormente, se estudiaron propiedades como la dureza, la rugosidad y las propiedades mecánicas de desgaste. En este estudio se obtuvo un recubrimiento más resistente.

Palabras clave:

Epoxi-poliéster, recubrimiento en polvo, hidrotalcita, resistencia al desgaste, Raman.

Index

Index of figures

1. Introduction

Organic coatings or paints represent one of the main solutions to protect different materials from corrosive phenomena, to which they are subjected by the working environment. Starting from recent years, the use of organic powder coatings has been developing rapidly, due to their good chemical and mechanical properties which guarantee greater durability, but also due to a lower environmental impact compared to liquid paints. In fact, liquid coatings are based on the use of solvents and waste products that contain toxic volatile compounds [1]-[3].

Furthermore, it is also important to underline an economic factor: in fact these coatings are cheaper for a series of reasons. The treatment of solvents is dangerous and requires precautions both from a production point of view due to their flammability, and for the operators who use them due to their toxicity. The powders, moreover, are reusable even when they are not applied [4].

Powder paints are composed of a solid resin that acts as a matrix, to which different types of solid particles can be added: additives; hardeners; organic and inorganic pigments; and stabilizers.

The application of the coating onto the samples can be carried out in several ways, always based on a common principle. The particles are electrostatically charged, often along the tube of the gun used for spraying, so that there is adhesion with the surface of the sample, subsequently crosslinking takes place in an industrial oven, heated to temperatures of about 150 – 200 °C. It is precisely the crosslinking reaction that transforms the powder paint into a continuous film over the substrate [4].

Nowadays, there are many research projects regarding organic powder coatings, this is due to the large number of advantages they involve.

1.1 Organic coatings

An organic coating can be described as a protective film formed by a continuous polymer matrix, commonly known as a binder, in which pigments and solid additives are dispersed. The coating is applied in liquid form to a metal substrate and then hardened to form a barrier against external agents [5].

It is defined as organic because the continuous phase, which forms the structure of the coating, is composed of carbon-based polymers or resins, such as epoxy, acrylic, or polyurethane resins, which give the film its fundamental adhesion and protective properties [6].

The main reason for using liquid organic coatings is to insulate the metal substrate from the surrounding environment, thus limiting the access of aggressive species that could trigger or fuel corrosion processes.

The way in which these coatings combat corrosion is based on a set of mechanisms: the first is the barrier function, which reduces the permeation of water, oxygen, and ions through the polymer matrix [5].

A second mechanism involves the presence of functional pigments, which can contribute to protection through phenomena such as ion exchange, in which aggressive ions are retained and replaced by counter-ions that can locally modify the conditions at the metal surface [7].

Another factor that has an impact is adhesion to the substrate, which plays an important role in limiting the propagation of corrosive phenomena under the film [6].

1.2 Organic powder coatings

Organic powder coatings can be defined as coating systems consisting of organic polymer matrices, pigments, fillers, and additives, applied in the form of a fine powder, which is then cross-linked in industrial ovens to form a continuous, protective film on the surface of the substrate [8].

Powder coating systems can be classified into two categories: thermoplastics and thermosets. Unlike thermoplastics, thermosetting resins have the characteristic of changing their properties as a result of cross-linking, which generally occurs at temperatures between 150–200 °C.

The protection provided by these coatings is based on the melting and coalescence of particles during baking, leading to the formation of a homogeneous film that helps to insulate the metal substrate from corrosive agents [9].

Powder coatings offer several significant advantages over traditional liquid organic coatings: they do not contain solvents, so there is no release of volatile organic compounds (VOCs) during application and baking.

In addition, the yield is close to 100% of the material applied, thanks to the possibility of recovering and reusing undeposited powders; in addition, they can reduce the production of hazardous waste, such as sludge from painting baths. Finally, they allow greater control of the thickness of the applied film, resulting in a reduction in surface defects [8],[10].

In terms of corrosion behavior, organic powder coatings provide protection comparable to, and in some cases superior to, liquid coatings due to their ability to form a continuous, non-porous film that acts as a physical barrier against oxygen, water, and aggressive ions [8].

Liquid organic coatings, due to the presence of solvents, can exhibit evaporation phenomena, generating microdefects or residual porosity in the film, while powder coatings, after cross-linking, exhibit better compactness and corrosion resistance [9].

Extensive research into organic powder coating systems has shown that the integration of functional pigments and corrosion inhibitors in powder coatings helps to increase their protective effectiveness, both through a barrier action and through chemical interactions with the substrate, which reduce the rate of corrosion [8].

The latest developments in bio-based powder systems have shown promising anti-corrosion performance, while maintaining the environmental and sustainability benefits that distinguish powder coatings from traditional liquid coatings [10].

There are many types of hybrid powder coatings, which are defined as such because they mix two or more polymer resins to balance mechanical and chemical properties. The most popular industrial formulations are epoxy-polyesters, polyurethanes, and modified acrylics.

Polyurethanes are particularly popular, especially for outdoor applications, because of their high resistance to weathering and UV rays; acrylics are good because they maintain gloss and color well over time. However, epoxy-polyesters will be used in this project because of their excellent chemical and physical resistance.

1.3. Failure mechanisms in coatings

The mechanisms of failure in organic powder coatings usually occur as a result of mechanical and environmental stresses, as the integrity of the protective film is compromised.

The process begins with the onset of localized defects such as scratches, cracks, or surface microfractures that interrupt the continuity of the coating, reducing the effectiveness of the barrier properties against oxygen, water, and aggressive ions [11].

The presence of these defects can trigger delamination, a mechanism whereby the adhesion between the coating and the substrate is progressively reduced starting from the edges of the defect. There are two different types of delamination: cathodic or anodic. In the case of cathodic delamination, the advancing front coincides with an active cathodic area, where the oxygen reduction reaction generates alkaline species that degrade adhesion. The anodic mechanism, on the other hand, involves the front developing at the anode, where metal dissolution weakens the interfacial bond [12].

Among relevant mechanisms to promote failure, abrasive wear stands out, which occurs when the coating is stressed by a harder material in relative motion, causing the progressive removal of the protective layer. This type of wear promotes the formation of microcavities and local loss of material, forming preferential pathways for the penetration of aggressive species [2]. Similarly, erosion induced by the repeated impact of solid particles generates a progressive thinning of the film and the formation of micro-cracks that accelerate the exposure of the substrate [13].

Damage and breakage of the coating have critical consequences for the substrate: it is from these exposed points that localized corrosion is triggered and propagates under the film through the delamination mechanisms described above. The process can be further aggravated when there is water absorption, oxygen diffusion, and chloride ions through defects and pores generated by wear [12].

In summary, organic powder coatings are effective as long as their ability to maintain film continuity and adhesion to the substrate is not compromised. The loss of these properties is the trigger for the failure mechanisms that lead to corrosion of the substrate they protect [14].

1.4 Functionalized organic powder coatings

Organic powder coatings functionalized with nanoparticles represent an important evolution compared to traditional organic coatings, due to the possibility of improving mechanical and chemical properties without the use of solvents, ensuring the possibility of reducing environmental impact and improving the durability and effectiveness of protected surfaces [14].

Various particles are used to functionalize organic powder coatings, including, for example, nanosilica (SiO_2) particles, which have been shown to be effective in increasing resistance to wear, scratching, and erosion due to their high hardness and chemical stability. The addition of nanosilica has resulted in a reduction in the depth and width of grooves in wear tests and a lower coefficient of friction compared to conventional organic coatings [2], [15].

These improvements are attributable to the increased hardness of the coating and greater resistance to plastic deformation of the matrix, an effect achieved through the hard nature of the nanoparticles and their homogeneous distribution [1].

Among the functionalizing particles, it is also worth mentioning silicoaluminates, SiAlON, Al_2O_3, and SiC, which contribute to increasing rigidity, scratch resistance, and impact resistance [1], [16].

Along with tribological properties, nanoadditives also provide better chemical resistance and greater dimensional stability under mechanical or environmental stress.

Using dispersion techniques such as ball milling or hot mixing, which ensure good dispersion, prevents the formation of surface defects (e.g., microcracks, porosity) that can be preferential pathways for the entry of corrosive agents [1], [18].

The latest research sees hydrotalcites, thanks to their layered structure and anion exchange capacity, as functionalizing particles with the potential to increase the corrosion resistance of coatings, acting both as a physical barrier and as a reservoir of anticorrosive species released in the presence of aggressive agents [16], [17]. The inclusion of hydrotalcites has also shown an improvement in surface hardness and scratch resistance, reducing delamination and improving adhesion to the substrate [16].

In conclusion, the properties of functionalized organic powder coatings are significantly superior to those of conventional organic coatings: greater resistance to abrasion, scratching, and erosion, better chemical and dimensional stability, and better anti-corrosive properties thanks to the distribution and effective interaction of nanoparticles with the polymer matrix.

1.5 Zwitterion-Hydrotalcite (ZHT)

These are lamellar compounds, better known as layered double hydroxides (LDH), composed of positively charged layers containing divalent and trivalent cations (e.g., Mg^{2+} and Al^{3+}), separated by exchangeable anions and water molecules.

Figure 1 shows a diagram of the typical lamellar structure of hydrotalcites, the general formula by which they can be represented is as follows:

$$[M^{2+}_{1-x}M^{3+}_{x}(OH)_2]^{x+} \cdot (A^{n}_{-})^{x/n} \cdot mH_2O$$

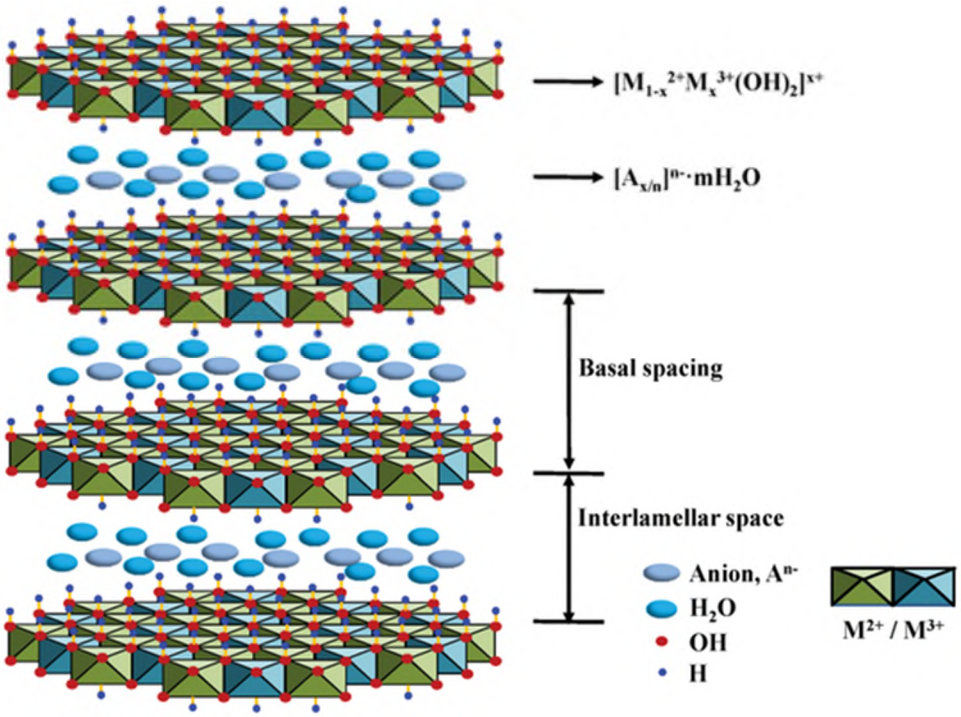

Figure 1. Diagram of the lamellar structure of hydrotalcites

Where A^{n-} is the intercalated anion, while x represents the molar fraction of trivalent cations [7].

In this project, as previously mentioned, a particular type of hydrotalcite was used: ZHT (Zwitterionic Hydrotalcite), obtained by modifying the surface of hydrotalcite with zwitterionic polymers such as sulfobetaine methacrylate (SBMA). The process takes place through reverse atom transfer radical polymerization (RATRP), which allows the bonding of groups containing both positive ($–NR_4^+$) and negative ($–SO_3^-$) charges to the surface of the LDH layers [18].

The reason why ZHT was used as an additive filler in the epoxy-polyester powder coating is because it was hypothesized that it could have some positive effects. Citing and analyzing a few of them:

- Favor a better dispersion of the filler, avoiding aggregation issues and improving surface morphology [7].
- Hydrotalcite can actually help with better dispersion, but this depends on the percentages in which it is added.Increase the hydrophilicity of the coating through its ability to retain water molecules [7], [18].
- This feature proved to be a double-edged sword during the development of the components. The moisture contained in the hydrotalcite can be harmful from the point of view of material aggregation. Removing the intrinsic moisture from the filler was one of the most challenging aspects of the project.
- Increase chemical resistance and stability in saline or acidic environments.

This is the core of the project. The goal is precisely to make the component functional in aggressive environments. It is unquestionably the central property in the development of coated steels for structural applications. [7], [18]

1.6 Raman spetroscopy

Raman spectroscopy is an analytical technique based on inelastic light scattering, which provides information on molecular vibrations. Its sensitivity allows for the study of chemical structure, internal stresses, and interactions at the micro and nanometric levels [19], [20]. This analysis is useful in polymer composite coatings, as Raman spectroscopy allows for non-destructive evaluation of residual stress distribution, inorganic filler dispersion, and the effectiveness of adhesion at the interface between the matrix and reinforcement. This technique has the characteristic of being able to detect micro-variations in the positions of Raman peaks, which are related to local deformations and stress states, allowing two-dimensional or three-dimensional maps of mechanical and chemical properties to be obtained, with sub-micrometric resolution and the possibility of in situ analysis of coatings on metal substrates, allowing non-destructive analysis [21], [22].

Unlike Raman spectroscopy alone, confocal Raman spectroscopy uses a confocal optical system that limits the collected radiation to the laser's focal region, thereby reducing signals from out-of-focus planes; the use of this technique allows precise chemical mapping of the distribution of phases and the dispersion of nanoparticles in organic coatings (and not only), thus enabling the monitoring of local changes due to abrasion or wear processes [23]. In such systems, Raman spectroscopy allows the shift of the characteristic bands of the polymer matrix and fillers to be measured, such as aromatic C–H vibrations or bands related to epoxy resin bonds, whose variations are important indicators of changes in the molecular structure or distribution of residual stresses [21], [24].

It is thanks to these characteristics that confocal Raman spectroscopy is a useful tool for studying the functionalization of coatings in an integrated manner.

2. Objective

The aim of this project is to analyze, using confocal Raman microscopy, the functionalization of the organic powder coating based on epoxy-polyester paint, using submicrometric hydrotalcite, present in quantities equal to 1 and 3% by weight, as well as to study the changes between the original coating and after abrasive wear tests.

To this end, several partial objectives have been carried out:

- Thermal analysis to evaluate the cross-linking process upon addition of the functionalizing filler (hydrotalcite).
- Surface morphology analysis to understand the quality and functionality of the coating.
- Evaluate the mechanical properties by performing universal hardness tests, to verify whether the addition of hydrotalcite causes variations in the hardness of the coating.
- Evaluation of abrasive wear using a tribometer, to focus more on the wear suffered by the coating and substrate.
- Confocal Raman spectroscopy is used to evaluate whether there are effects on the stress distribution of the polymer when hydrotalcite particles are added; furthermore, the objective is to evaluate whether there are stress states caused by abrasive wear, to compare the original coating and after functionalizing it.

3. Experimental procedure

3.1 Materials and preparation

In this work, a FF22 thermosetting semimat powder coating based on epoxy and polyester resins was used, provided by Iba Kimya; while a additive charge was used a Mg-Al-Zn Hydrotalcite (ZHT-4V), provided by Kisuma Chemicals B.V.

The development to functionalize this coating initially involved a preheating of the components, both the hydrotalcite and the EP-PE coating to remove any humidity that the materials may contain.

Focusing on the ZHT, it was placed in an oven at a constant temperature of 85°C for no less than 12 h, with the aim of removing the moisture to which the material is intrinsically subject, which could cause aggregation problems during the coating phase.

The EP-PE powder coating, on the other hand, was brought to lower temperatures, around 40°C, with the ultimate goal of removing residual moisture and increasing miscibility with the additive filler.

Table 1. Nomenclature of materials used

Sample	Weight percentage of Zwitterion-Hydrotalcite nanoparticles (%)	Nomenclature
Epoxy-polyester coating	0	EP-PE
Epoxy-polyester coating with hydrotalcite	1	1% ZHT
	3	3% ZHT

Subsequently, it was decided to divide the weighed portions into 50 g portions, so that ultrasonic dispersion techniques could be performed more effectively, in order to avoid agglomeration or poor distribution of the filler additive.

As shown in Table 1, mixtures with different concentrations of hydrotalcite were prepared: 1% and 3% by wt.

The mixing system used was an ultrasonic system (Resodyn), which enables a level of dispersion homogeneity that traditional mechanical mixing systems struggle to achieve.
The process was carried out on each 50 g sample (powder coating + hydrotalcite) for 30 s at 60 Hz, consistently yielding g values above 97, a clear indicator of the mixing process being performed.
It is necessary to specify that even the EP-PE powder coating alone was subjected to ultrasonic mixing to obtain samples that underwent the same processing conditions.
The coating was applied to rectangular carbon steel samples with the following dimensions: 152x76x0,8 mm; the steel components were previously cleaned with ethylene and then sanded with sandpaper. This procedure aimed to make the surface rougher and more suitable for better adhesion with the hybrid coating.
The painting was carried out in a semi-industrial booth using an electrostatic gun Pulverizadora Manual Easyselect, with a voltage source of 100 kV applied. The polymerization process, as indicated by the manufacturers of the powder paint, was carried out in an oven at 180 °C for 15 min, thus obtaining the painted sample.

3.2 Coating characterization

3.2.1 DSC analysis

The DSC (differential scanning calorimetry) analysis technique is based on measuring the heat flow difference between a substance and a reference as a function of the temperature difference. In this analysis, both the substance and the reference are subjected to a controlled temperature program [25].
Through the DSC technique, it is possible to obtain information regarding glass transition temperature (Tg); the output will be a graph whose areas under the peaks (maximum and/or minimum) represent the transition enthalpies of the material under examination [25]. In this project, the glass transition temperature was evaluated to determine if and how it varied with an increase in hydrotalcite percentage.
Three tests were conducted for each composition, and each test involved approximately 10 mg of sample; the analysis was performed with a heating rate of 20 °C/min, bringing the sample from a temperature of 25 °C to a final temperature of 200 °C.

Furthermore, for the calculation of the Tg, coating fragments of the thickness of the entire coating were used.

3.2.2 Roughness

In order to measure the roughness, Opto-digital Olympus DSX500 (Olympus Corporation, Tokyo, Japan) optoelectronic microscope was used, which allows the measurement of both linear roughness (Ra) and surface roughness (Sa).

Three images were acquired for each composition, on each of which twenty measurements of the Ra parameter were taken, for a total of 60 measurements for each mixture. With regard to the Sa parameter, three images were taken for each composition, with one measurement per image, for a total of three measurements per coating mixture.

Ra values were measured by taking ten vertical lines and ten horizontal lines randomly distributed over the surface of the sample. Surface roughness, on the other hand, was measured by taking only one randomly selected value.

All measurements were repeated three times for each composition (EP-PE, 1%, and 3%).

Furthermore, to visually support the data collection, three-dimensional images with a color scale were acquired.

3.2.3 Abrasive wear

Abrasive wear occurs when, between two bodies in contact and relative motion, there is a progressive removal of material from the softer surface [26]. In this project, abrasive wear was carried out using UMT Tribolab (Bruker, Massachusetts, USA) tribometer, under dry conditions, without lubricant, and whose counter-material is a stainless-steel ball with a diameter of 6 mm.Four tests were performed in each organic coating at 10 N applied load, during 5 min at a frequency of 5 Hz.

Following the tribological test, using an Olympus DSX500 optoelectronic microscope, the traces left by the tribometer were evaluated, both in-depth and in width. Each of the four traces left on each sample was analyzed; ten measurements were randomly collected longitudinally to evaluate the depth and twenty measurements to evaluate the width.

In this way, by assessing the variation in the size of the imprint, it was possible to evaluate the variation in damage for the different percentages of ZHT.

3.2.4 Universal hardness

Universal hardness, in the field of coatings, can be an excellent indicator of the mechanical properties obtained and of how the fillers have functionalized the coating, sincethe hardness data can be correlated with the sample's behavior under abrasive wear.

This type of test is carried out using a diamond cone, which makes an indentation on the surface of the sample without however breaking the coating.

The goal is to measure universal hardness (HM), plastic hardness (HUplastic), and stiffness (YHU).

Universal hardnessmeter ZHU 2.5 (Zwick Roell, Ulm, Germany) was used. The applied load was 5 N, the speed load application was 1 mm/min and the speed load removal was 10 mm/min. Twenty measurements were carried out on each organic coating.

Further information obtained from this test includes the Wtotal values, namely the total indentation work, which corresponds to the sum of the plastic work (Wplast), which is non-recoverable, and the elastic work (Welast), which is recoverable.

This information was obtained by evaluating the distribution of mechanical energy absorbed by the material as a function of the penetration depth "h," which is considered when the hardness tester applies the maximum force, Fmax [27], [28].

In Figure 2, a force–depth graph is shown, whose curve includes the components of total, plastic, and elastic work.

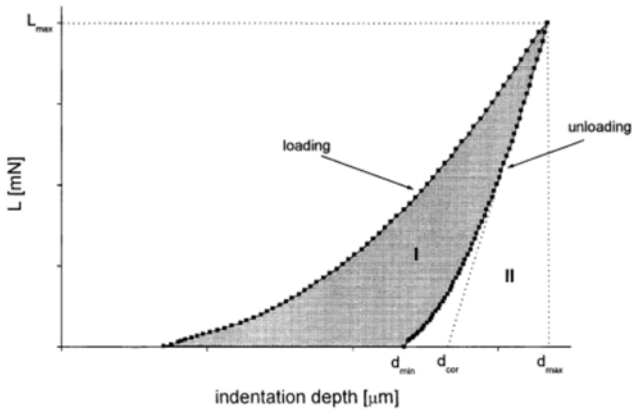

Figure 2. Force-Penetration plot

3.2.5 Raman analysis

A high-resolution Witec Alpha 300RA confocal Raman microscope (Witec, Germany) equipped with a 50X magnification lens was used for the analyses, as shown in Figure 3.
The Raman measurements were performed using an excitation laser with a wavelength of 532 nm, with an optical fiber collection diameter of 50 µm and a power of 3.7 mW. The scanning areas for acquiring the Raman images were 25 × 25 µm, with a 50 × 50 pixel grid (0.5 µm pitch). The integration time for each spectrum was 0.3 s. The collected spectra were processed using Witec Control Plus software (Ulm, Germany). Before proceeding with data analysis, preliminary treatments were applied for cosmic ray removal (CRR) and background subtraction (BSub). Three maps were acquired for each sample in order to obtain a representative view of the organic coatings. The spectral resolution achieved was 0.05 cm^{-1}.
It is important to specify that the spectral analysis is normally performed using Lorentzian fitting, a method that allows to model the spectral peaks with Lorentz functions to determine with high precision the position, intensity and width of the bands, and also to identify minimal displacements (of the order of 0.01 cm^{-1}) useful to correlate the chemical properties with the mechanical and tribological characteristics of the coating [21], [22].

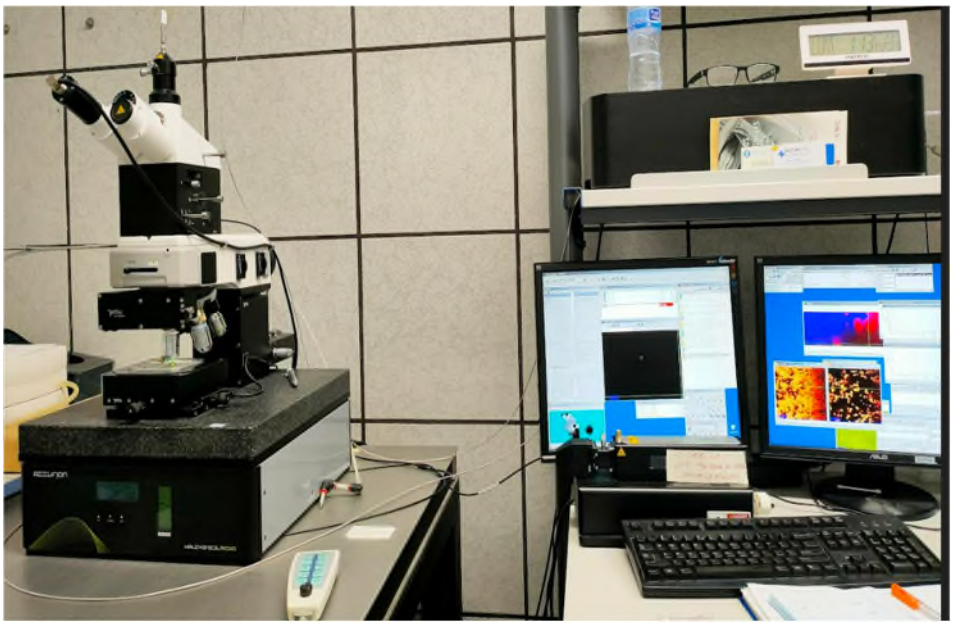

Figure 3. Witec Alpha 300 RA High Resolution Confocal Raman Microscope (Witec, Germany)

4. Results

4.1 DSC

The Tg is calculated by considering the points of intersection of the tangents between the point where the heat flow begins to deviate, indicating the start of the glass transition, and the point where the heat flow stabilizes again, indicating the completion of the transition; Figure 4 shows some DSC curves to better understand how the glass transition temperature was calculated.

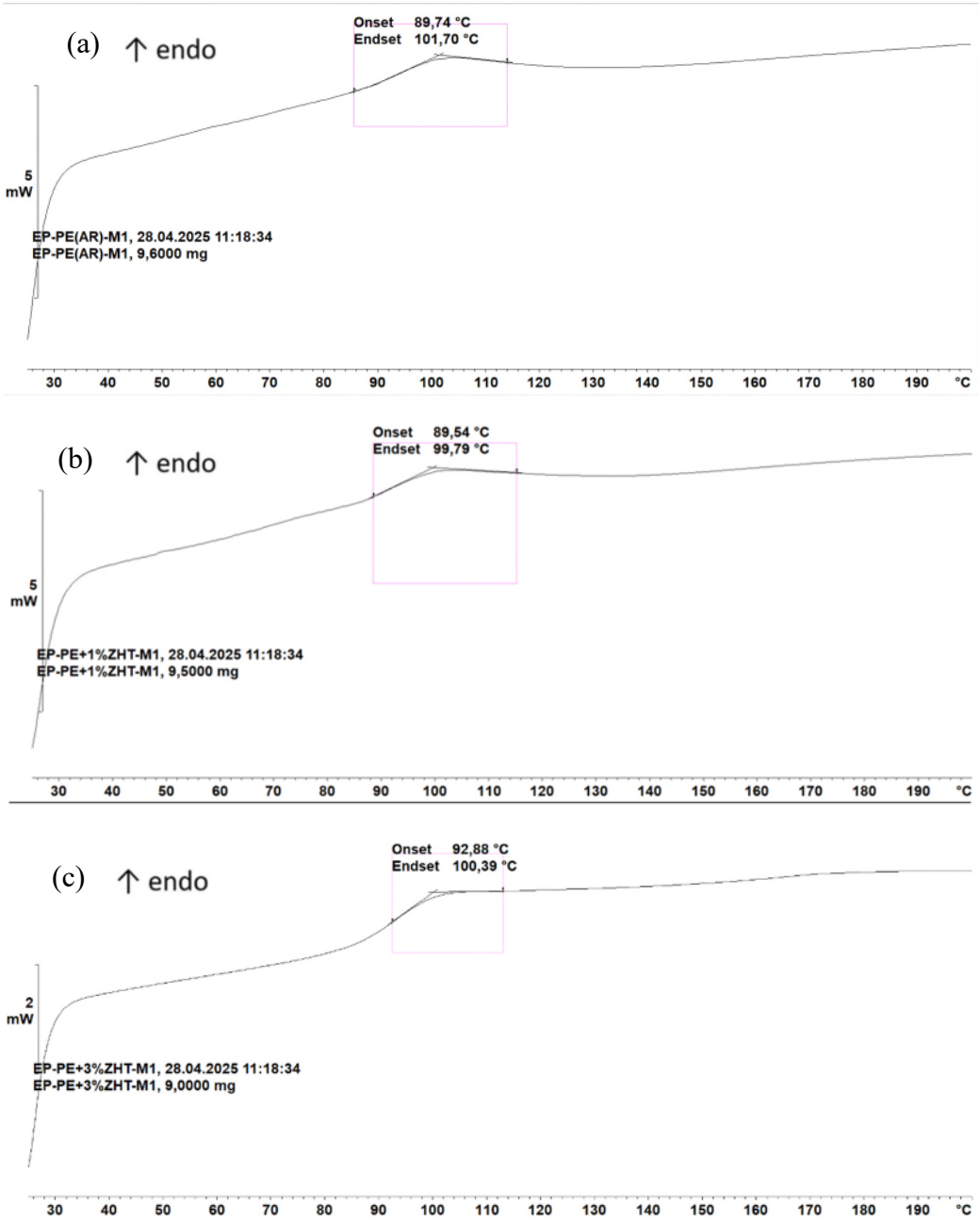

Figure 4. Thermograms: a) EP-PE; b) 1% ZHT; c) 3% ZHT

Tg is a parameter related to the cross-linking of polymer chains; in fact, an increase in the Tg of a polymer reinforced with additive fillers is correlated with a good degree of cross-linking, attributed to the increase in the interfacial area between the particles and the polymer chains [29].

Figure 5 shows the Tg values of all organic coatings obtained by DSC, it can be seen that the Tg for EP-PE paint alone corresponds to 96.6 °C, while following the addition of hydrotalcite it corresponds to 97.0 °C for 1% ZHT and 96.7 °C for 3% ZHT.

In the case under examination, there is no increase in Tg, which remains approximately constant, highlighting good distribution in the matrix, since if there were agglomeration phenomena, a decrease in the glass transition temperature would have been observed [29].

Furthermore, the fact that the Tg does not increase significantly can be attributed to a restriction in the mobility of the polymer chains in the vicinity of the ZHT particles, the physical interactions between the matrix and the filler could locally limit the movement of the chains, maintaining the cost or slightly increasing the Tg [30].

Moreover, the filler can contribute as a physical cross-linker, increasing the local stiffness and the apparent degree of crosslinking of the polymer [31].

However, the absence of a further increase in Tg at 3% suggests a saturation effect: beyond a certain threshold, the additional particles do not further improve the interaction with the matrix, perhaps due to aggregation or poor dispersion. As a consequence, the effectiveness of the filler in confining the polymer chains stabilizes, leading to a Tg similar to that of the system with 1% ZHT.

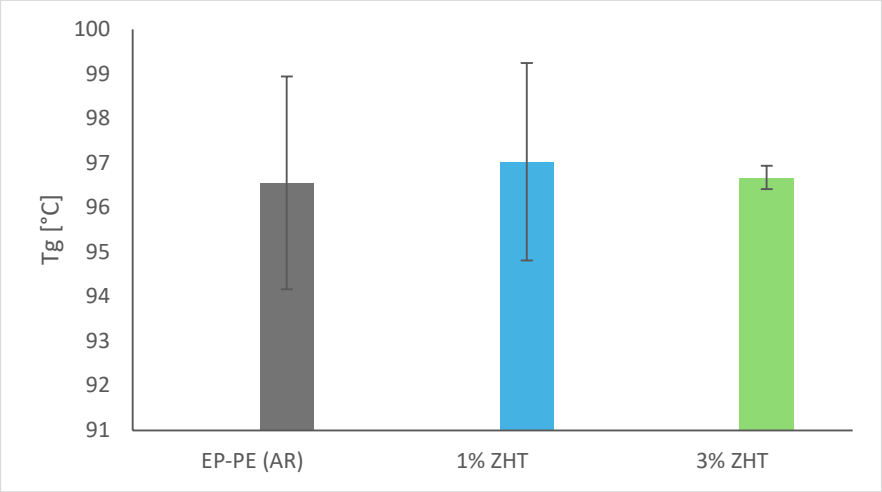

Figure 5. Glass transition temperature for different types of paints

4.2 Roughness

In Figure 6 the values of Ra and Sa are represented, as it can be seen, there is an increase in roughness with the addition of hydrotalcites.

It is observed that as the hydrotalcite content increases, the formation of aggregates on the surface after deposition increases, and these aggregates remain even during cross-linking.

This phenomenon can be explained by the fact that as the concentration increases, particle-particle interactions also increase, resulting in the aggregation of the particles.

Furthermore, aggregation is attributed to the hexagonal lateral dimension of the hydrotalcite platelets, since when they are large, the surface charge is not uniform and they tend to attract each other laterally [32].

It is not possible to discard the hypothesis that the higher the hydrotalcite content, the greater the formation of aggregates on the surface after deposition, i.e. the aggregate formed on the substrate after the removal of the sample from the solution; if this hypothesis were true, the aggregation should not be too large since it is not observed in the Tg.

Another factor that can influence the increase in surface roughness is the shape of the additive filler; in fact, spherical shapes provide good surface homogeneity compared to irregular or lamellar shapes.

The addition of a filler such as hydrotalcite, due to its lamellar shape, could protrude from the surface, resulting in an increase in surface roughness. [33]

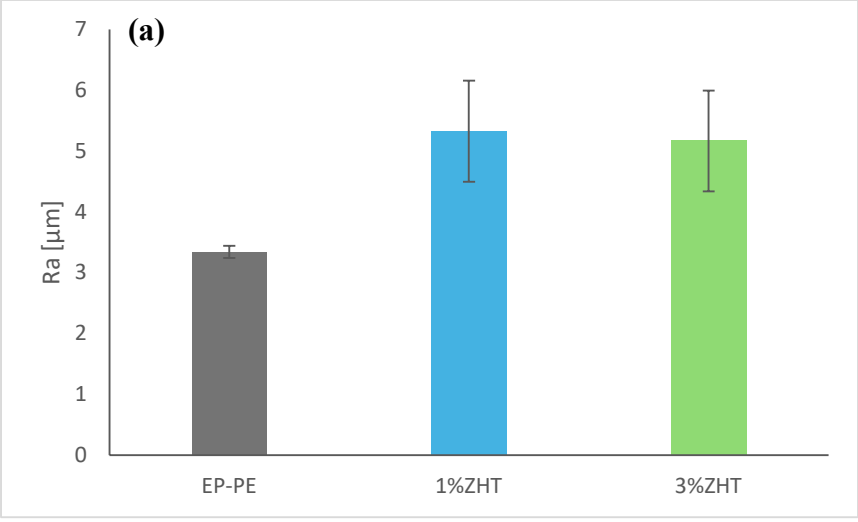

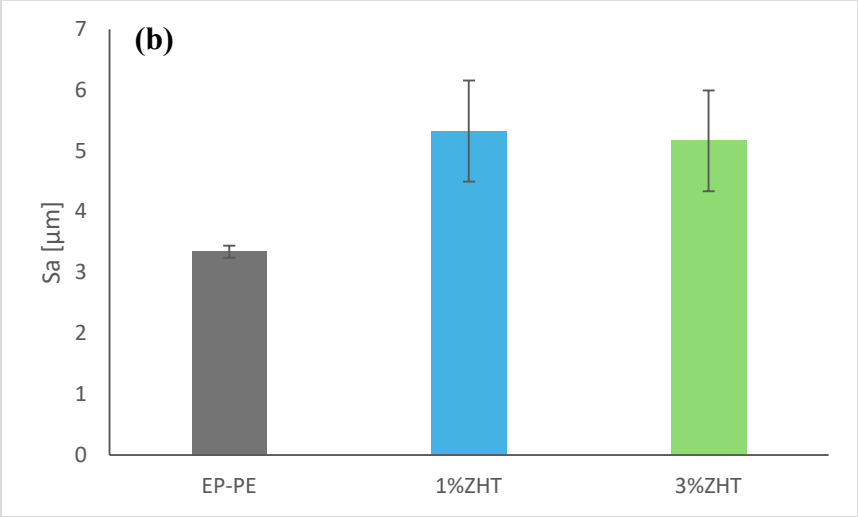

Figure 6. a) Ra and b) Sa of all organic coatings

4.3 Universal hardness

The universal hardness test made it possible to obtain the values of universal hardness (HM), plastic hardness (HUplast), and the plastic modulus (YHU).

It can be observed in Figure 7 that the values of HM, are higher for the sole EP-PE coating, while they decrease for the hybrid coating in which ZHT hydrotalcite is added; this indicates that the universal hardness is greater for the powder coating without the presence of additive fillers.

This trend can be attributed to the interference that hydrotalcite could exert in the crosslinking process, since it is basic in nature (contains anions such as carbonate or hydroxide between the lamellae), during chemical interaction with the functional groups of the resin, it neutralizes the acidic groups of the polyester or binds to the additives/catalysts [34].

In case hydrotalcite does not bring direct improvement in the degree of crosslinking the hardness would also be a function of the intrinsic hardness of the additive filler, it can be proven through the product data sheet that the added hydrotalcite has low Mohs hardness values.

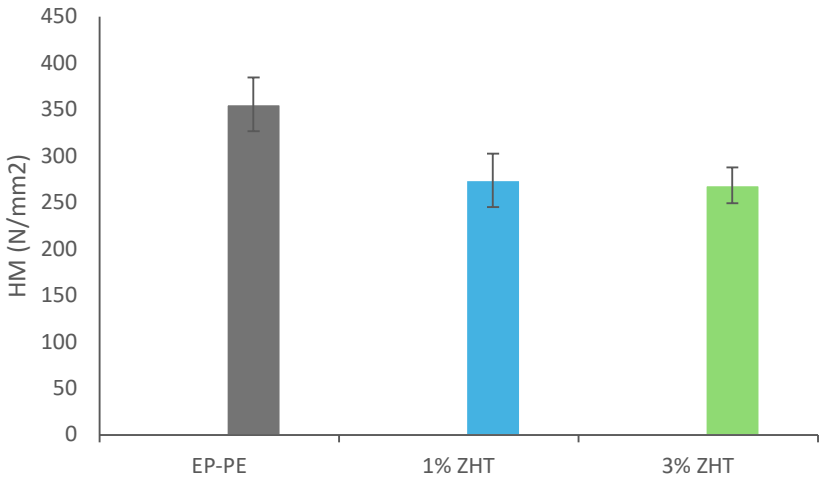

Figure 7. Universal hardness values

Further results, shown in Figure 8, relate to the total work (Wtotal), elastic work (Welas), and plastic work (Wplas).

It can be observed that the values of total, elastic and plastic work increase with the increase in the percentage of hydrotalcite; the indenter required more energy to penetrate the material because the latter absorbs more overall mechanical energy; in other words, the material turns out to be more ductile.

It is interesting to note how the total work for 1% ZHT and 3% ZHT is almost the same, highlighting how the mechanical behavior does not vary significantly with the increase in hydrotalcite percentage.

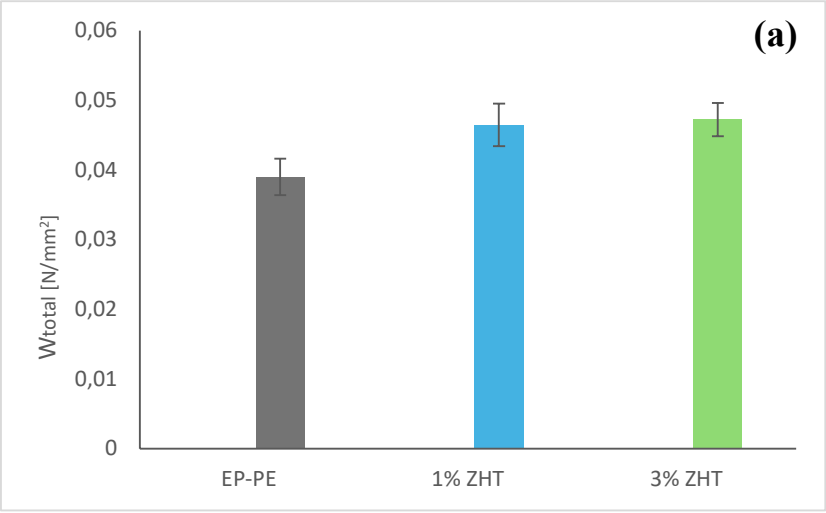

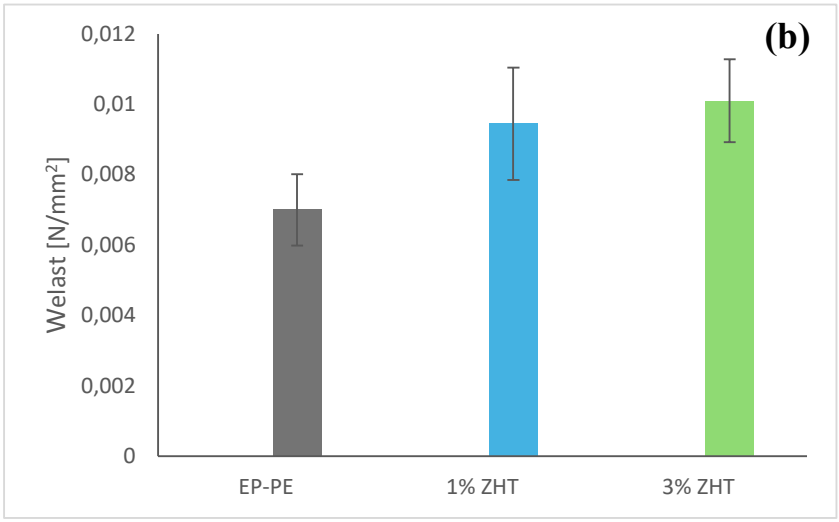

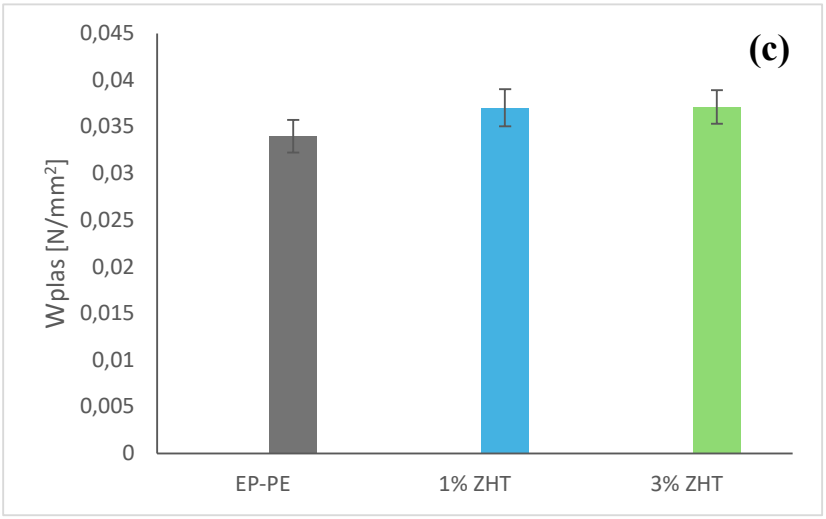

Figure 8. a) total wor; b) elastic work; c) plastic work

4.4 Abrasive wear

The Figure 9 displays the coefficient of friction behavior of each coating analyzed at a load of 10 N.

The friction coefficient (COF) denotes the relationship between the displacement and friction forces of two surfaces when they come into contact with each other.

In the COF curvse, up to three different wear phases can occur over time, depending on the nature of the material. The first phase involves a COF that starts at low values and gradually increases over time (a mechanism associated with sliding conditions), the second phase is characterized by a rapid increase in COF (a symptom of the onset of abrasive wear), and finally, a last phase in which the curve stabilizes at high COF values, while remaining constant.

Figure 9 shows that for both EP-PE paint alone and hydrotalcite coating, the first phase, relating to sliding, is present but minimal; this indicates that the wear phase occurs a few seconds after the start of the test. However, it should be noted that the samples containing hydrotalcite show a slight delay in the curves compared to the paint alone, indicating that the sliding phase persists for longer.

Considering the COF values and the trend of the curves, it can be said that the predominant part of this wear test is the abrasive part.

However, greater hardness does not necessarily indicate better wear behaviour. High hardness can be synonymous with greater fragility of the coating, causing an increase in the worn surface [1], [35].

Through its lamellar structure, hydrotalcite acts as a solid lubricant, forming micro-barriers that reduce friction and wear depth. [1], [36]

Based on the behavior of the curves shown in Figure 9, it is possible to state that the paint composition containing 3% ZHT is the mixture that shows the best wear properties.

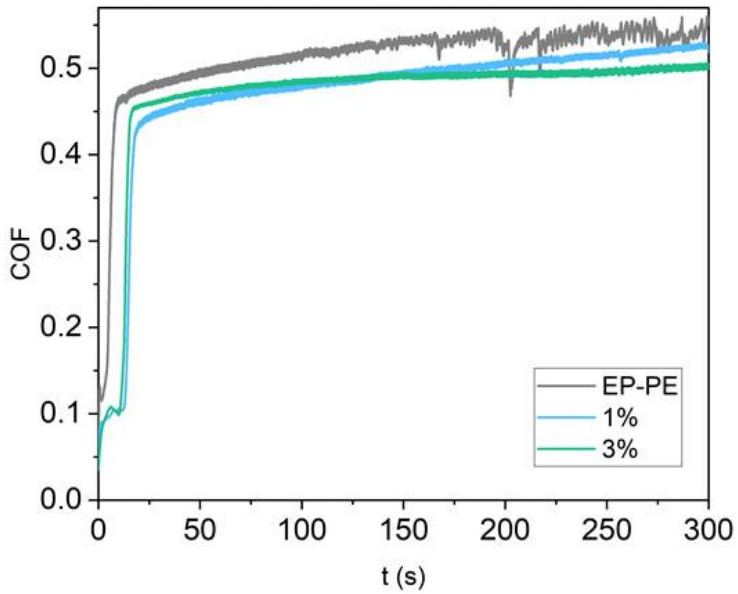

Figure 9. COF evolution of all oprganic coating for each paint

In order to support the wear data, color images of the imprint left by the tribometer were taken, shown in Figure 10; the color scale goes from 0 to 150 µm and the blue color indicates a greater depth reached, it is therefore possible to notice how as the percentage of hydrotalcite increases the coating becomes more resistant to wear. The COF shows that the HT samples lift later and that their abrasive COF is lower, suggesting less material loss.

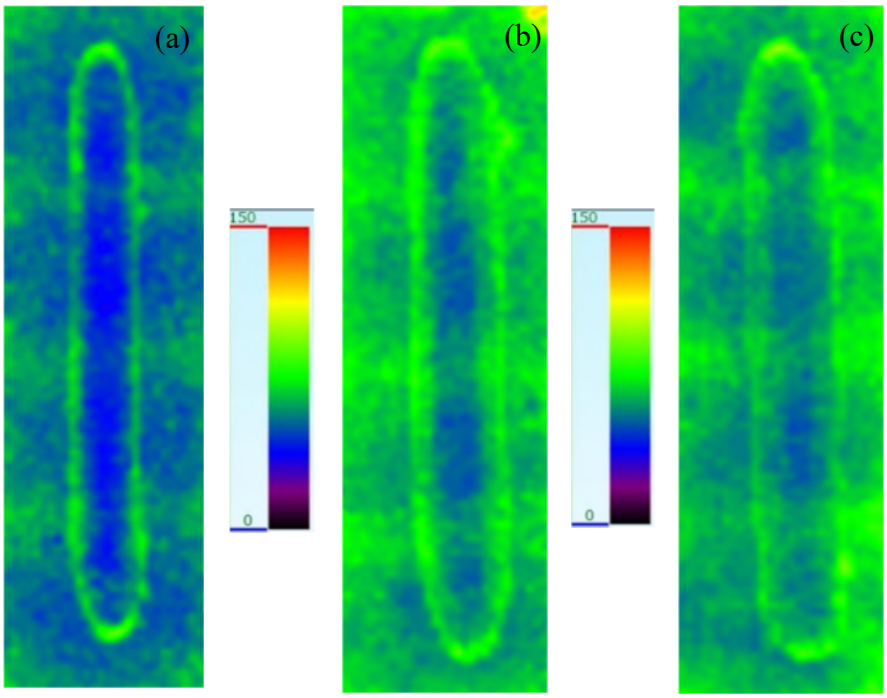

Figure 10. Color images obtained with the perfilometer: a) EP-PE; b) 1% ZHT; c) 3% ZHT

4.5 Confocal Raman Microscopy

The first step was to analyze the Raman maps obtained to identify the characteristic spectra and identify the elements that make up the commercial coating.

The analyses revealed two different of Raman spectra, in Figure 11. The first Raman spectrum identified relates to barium sulfate ($BaSO_4$, green in color), while the second relates to epoxy-polyester polymer (EP-PE, blue in color).

- To obtain Raman phase maps, the characteristic Raman bands of each material were integrated in order to represent the spatial distribution of these components:The band at 992 cm^{-1}, typical of barium sulfate, was integrated to locate the $BaSO_4$ particles [37].
- The band at 3070 cm^{-1}, related to the C-H functional groups typical of epoxy-polyester polymers, was integrated to highlight the distribution of the polymer matrix [21].

With the aim of proceeding with integration, the acquired Raman spectra were pretreated to eliminate cosmic rays (CRR) and correct the spectral background (BSub). These operations are essential to ensure that the calculated integral actually represents the contribution of the material of interest and not noise or instrumental effects.

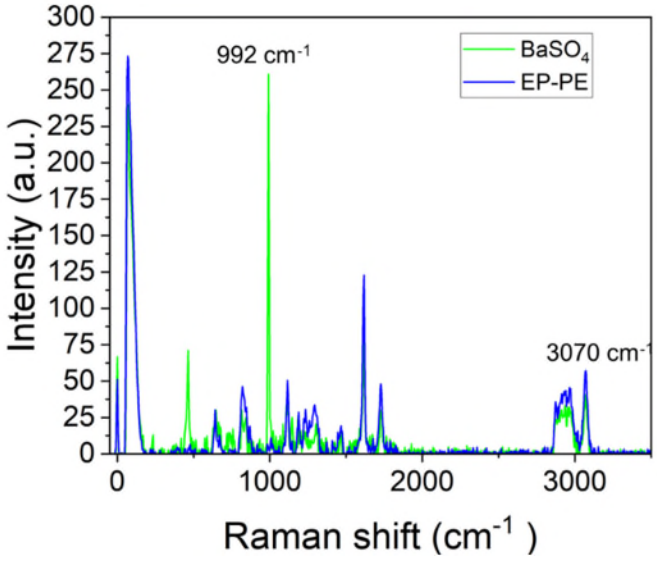

Figure 11. Average Raman spectra of raw materials

In addition, it should be noted that Raman spectra could not beobtained for hydrotalcites, as this material has no appreciable Raman effect under the measurement conditions adopted [20].

Figure 12 shows, for each coating, the Raman phase maps and the Raman shift maps related to the two characteristic bands analyzed in this work: 3070 cm^{-1} (central columns) and 1615 cm^{-1} (right columns). These bands have been chosen because they are associated with the C–H stretching vibrations (3070 cm^{-1}) and with the aromatic C=C stretching (1615 cm^{-1}), representing important markers of the organic matrix and its interaction with the inorganic filler. It is important to underline that the spatial distribution and the shift of these bands provide data on the chemical homogeneity, on the phase dispersion and in particular on the local stress states inside the coating, ensuring answers regarding the functionalization of the coating and the presence of hydrotalcite. [22], [23].

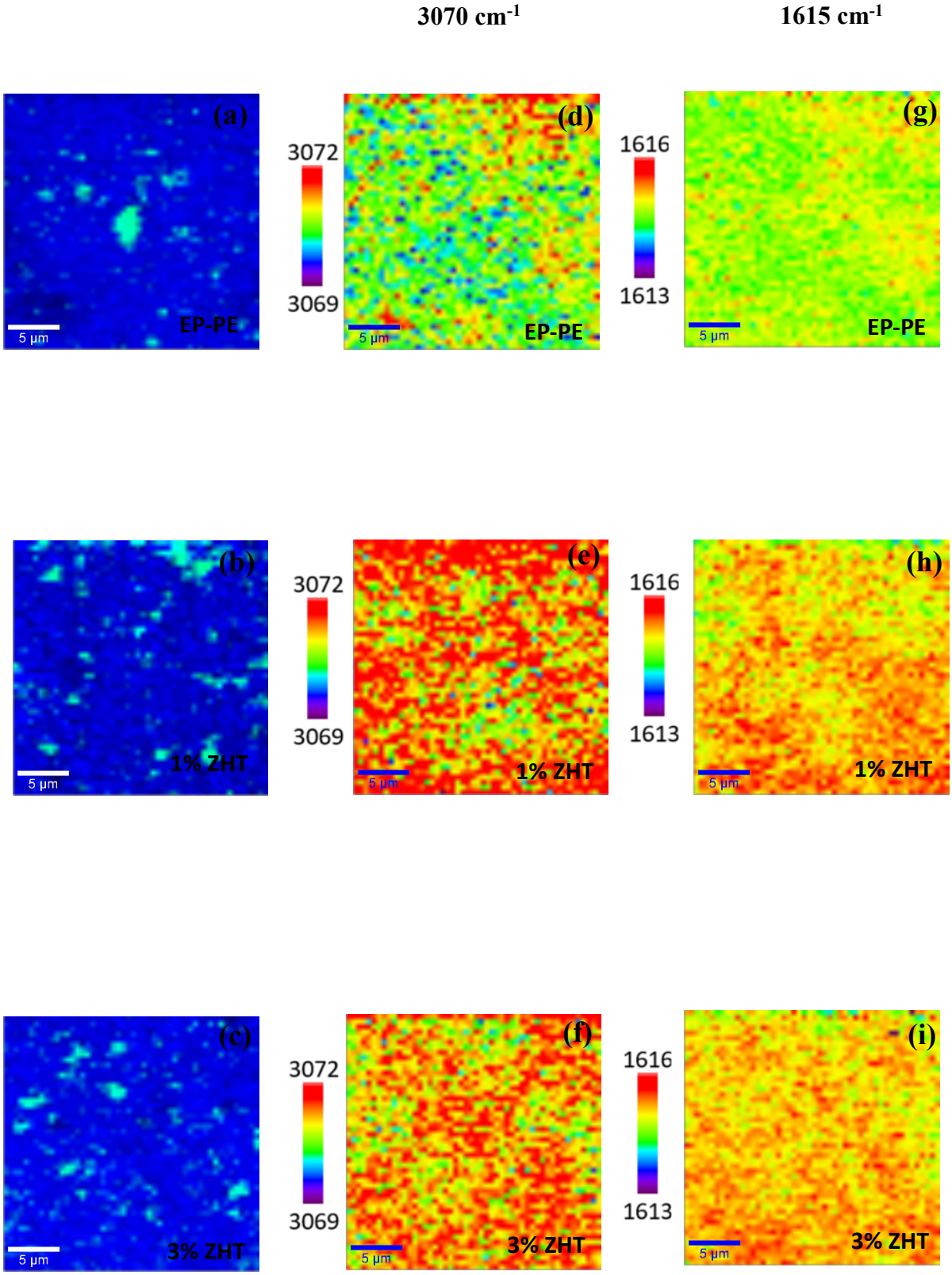

Figure 12. Images a), b) and c) represent the phase maps of the raw material. Images d), e) and f) represent the shift maps of the 3070 cm^{-1} band of the raw material. Images g), h) and i) represent the shift maps of the 1615 cm^{-1} band of the raw material.

Referring to the phase maps, Figure 12 a), b) and c), it is interesting to note how the distribution of $BaSO_4$ is relatively homogeneous; there do not appear to be any evident agglomerates.

Continuing with the analysis of the obtained results, Figure 12 shows the shift map of the bands at 3070 cm^{-1}, evaluated outside the wear mark; evaluating the values for EP-PE, 1% ZHT, and 3% ZHT for the 3070 cm^{-1} band, it is interesting to note that the epoxy-polyester paint shows the band is not affected by compression or tension phenomena.

Conversely, the analyses carried out on the paint containing 1% ZHT and 3% ZHT have shown that, although these components have not undergone mechanical testing, the Raman band exhibits compression phenomena, shifting to values around 3072 cm^{-1}.

This phenomenon may be the result of an increase in the degree of crosslinking, as the presence of inorganic fillers can enhance the polymer's degree of crosslinking. Some additive fillers may act as catalysts, resulting in a higher degree of crosslinking and consequent stiffening of the bonds within the polymer chain [21], [23].

Another possible cause is attributable to geometric constraints; rigid fillers can increase the elastic modulus of the matrix and significantly reduce chain mobility, as these fillers function as geometric constraints.

The polymer segments are confined between nanoparticles, and this can cause a state of pre-compression, preventing the bonds from “relaxing.”

Furthermore, hydrotalcite tends to decrease the relaxation of polymer networks, introducing micro-compression stresses [24]. The reasoning developed for the 3070 cm^{-1} band is equally applicable to the 1615 cm^{-1} band.

Figure 13 shows the pixels distribution associated with the two bands (3070 cm^{-1} and 1615 cm^{-1}) in the raw material case, these values are useful to give a quantitative idea of the pixels present at the corresponding band values, to quantify the Raman shifts of each area, the number of pixels is plotted against their Raman shift.

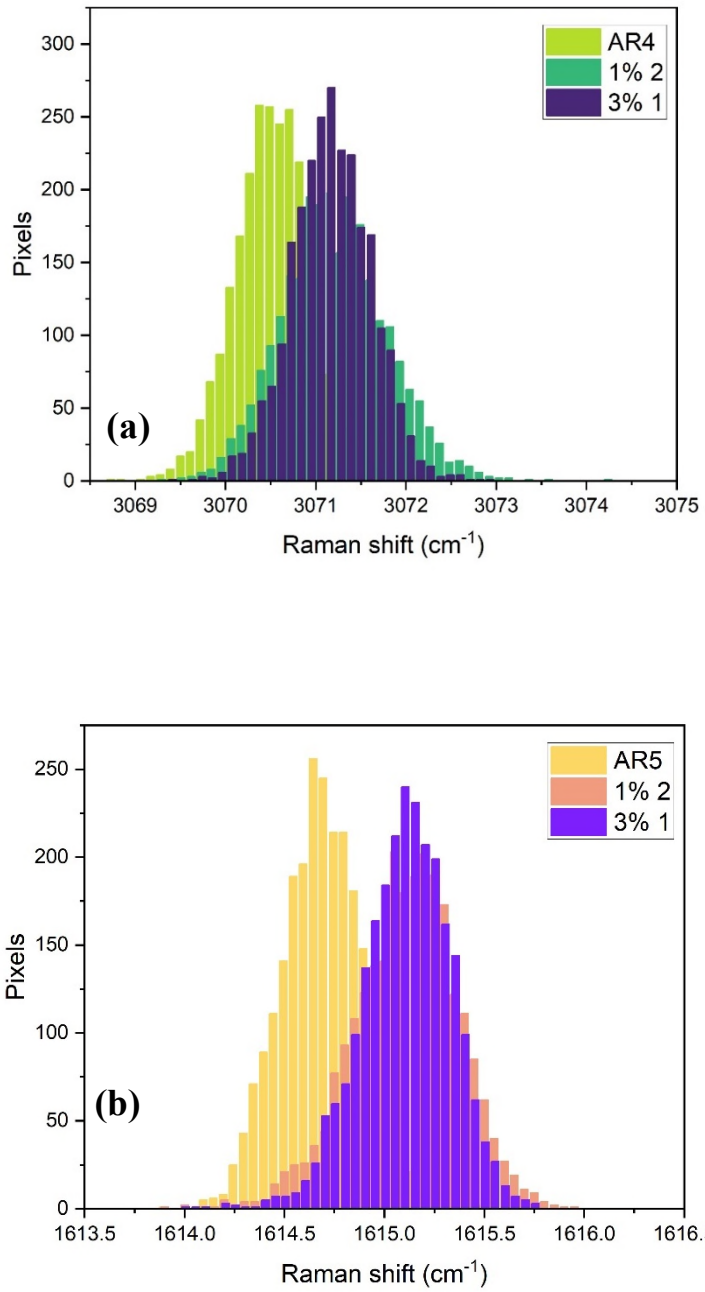

Figure 13. Raw material plot of pixels for: a) 3070 cm^{-1} band; b) 1615 cm^{-1} band

Figure 14 shows, for each coatings, the phase and shift maps for the two bands considered: 3070 cm-1 (middle column) and 1615 cm-1 (right column).

The results, obtained by Raman analysis, refer to the areas inside the wear track.

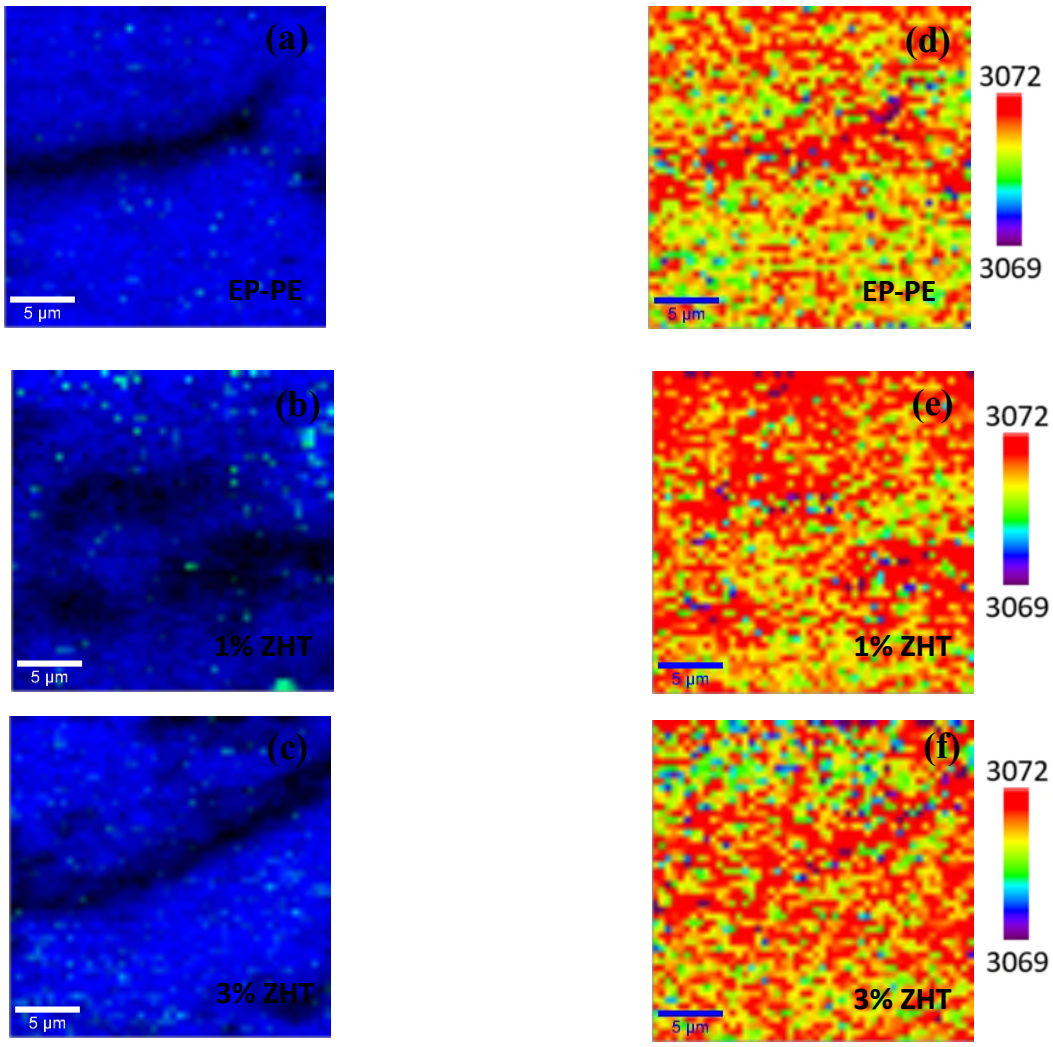

Figure 14. Images a), b) and c) represent the phase maps related to the wear track. Images d), e) and f) represent the shifts maps of the 3070 cm-1 band of the wear track.

In figure 14, images a), b) and c), show the phase map of $BaSO_4$ inside the track obtained following the tribological test, it is interesting to note how the barium sulphate, due to wear, has broken down into smaller components, this is due to the breakage of the pigments. [37]. Furthermore, the black areas that appear in the phase maps, called "crack", are due to the absence of polymer caused by the tribometer. In the absence of polymer, the Raman signal disappears or is practically non-existent.

In Figure 14, images d), e) and f), the shift maps corresponding to the 3070 cm^{-1} band related to the wear track are shown, thus considering the behavior inside the mark left by the

tribometer. In this case, the fact that the band shows a compression behavior is attributable to the mechanical wear stress caused by the tribological test.

The abrasive interaction locally deforms the surface; in fact, the aromatic C-H band may have moved from its original position, this indicates the presence of residual stresses in the case under analysis, compressive [22].

Figure 15 shows the pixels distribution associated with the two bands (3070 cm^{-1} and 1615 cm^{-1}) in the wear track case, these values are useful to give a quantitative idea of the pixels present at the corresponding band values.

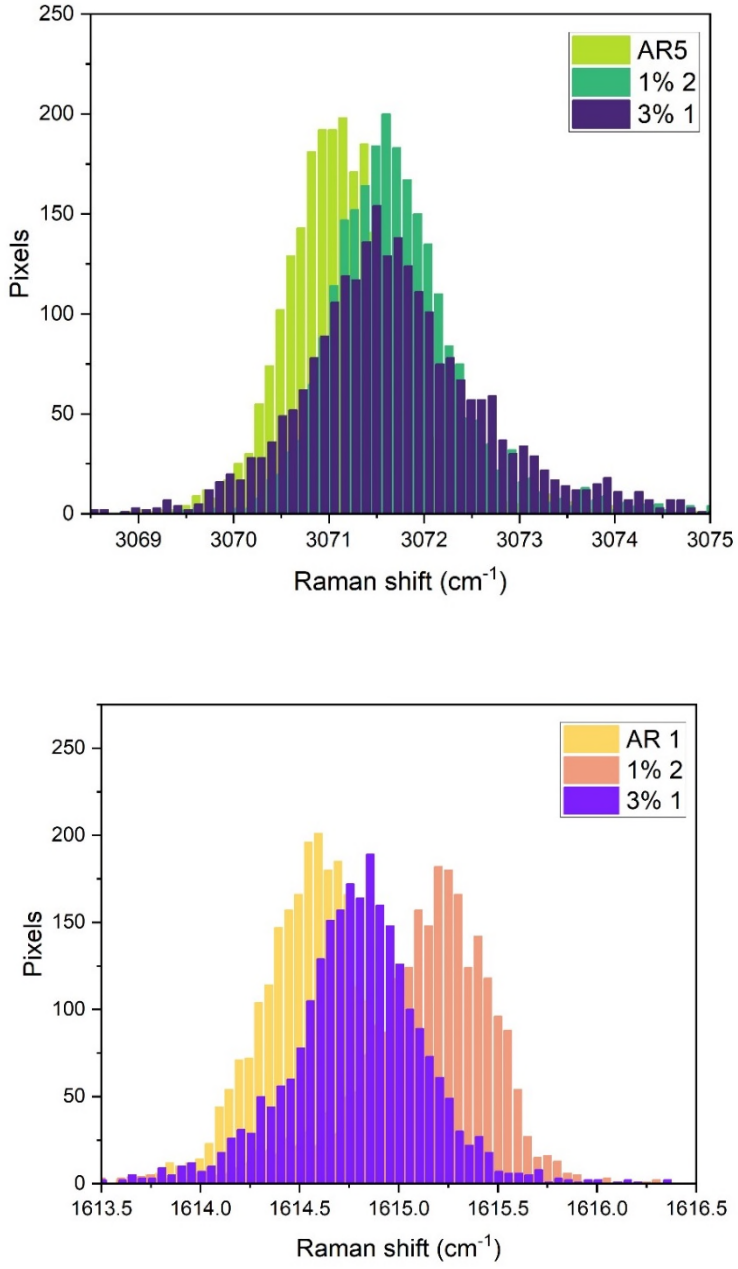

Figure 15. Wear track plot of pixels for: a) 3070 cm^{-1} band; b) 1615 cm^{-1} band

5. Conclusions

The conclusions obtained through the work carried out in this study can be summarized in the following points:

- The integration of the hydrotalcite nanoparticles within the epoxy-polyester paint was good; based on these assumptions, it was possible to obtain a uniform and homogeneous coating.
- The addition of hydrotalcite does not cause a change in the glass transition temperature, in fact the samples following the tests do not show any changes in this sense.
- The surface characteristics of the coating change as the additive filler is added; in fact, there is a significant increase in roughness, which increases as the nanoparticle content increases.
- Coatings containing hydrotalcites show improved abrasive wear resistance compared to commercial EP-PE paint; this is due to the reinforcing effect of the hydrotalcite particles, which ensure better load transfer within the matrix and delay abrasive contact, increasing wear resistance.
- The hardness values obtained indicate that the addition of hydrotalcite resulted in a decrease in hardness; in response, an increase in plastic work was recorded for the coatings containing additive filler, indicating that more energy is required to deform them.
- The confocal Raman microscopytechnique made it possible to assess the mechanical behavior of the coating in a timely manner, ensuring that it was possible to observe how the stretch of chemical bonds varied as a result of wear experienced by the component.

6. Future works

Following the work done, it could be interesting to carry out some future works, with the aim of expanding and integrating the knowledge on the functionalization of hybrid organic powder coatings. The following points are suggested:

- Evaluate other wear tests, for example Sandblasting test at 45°, in order to observe the behavior of the coating in other mechanical tests.
- Evaluate the corrosion protection of the coating by means of salt spray tests.
- Study a greater number of bands by means of Raman spectroscopy, in order to see how the functionality of the coating is influenced or how other functional groups respond to wear damage.
- Validate the use of Raman spectroscopy also with other coatings, of other organic nature.
- Investigate the possibility of adding other additive fillers, which are compatible with Raman analyses.

References

[1] Fernández-Álvarez, M. *et al.* (2020) 'Functionalizing organic powder coatings with nanoparticles through ball milling for wear applications', *Applied Surface Science*, 513, p. 145834. doi: 10.1016/j.apsusc.2020.145834.

[2] Fernández-Álvarez, M., Velasco, F. and Bautista, A. (2020) 'Epoxy powder coatings hot mixed with nanoparticles to improve their abrasive wear', *Wear*, 448–449, p. 203211. doi: 10.1016/j.wear.2020.203211.

[3] Calderón-Perea N.E., Velasco F., Bautista A., Fernández-Álvarez M. Hybrid coatings with hydrotalcites: A study on the mechanical properties. *Universidad Carlos III de Madrid & Instituto de Cerámica y Vidrio (CSIC), Spain*.Stoller, R. (1978) 'Electrostatic painting', American Journal of Physics, 46(4), pp. 435–436. doi: 10.1119/1.11320.

[4] Lyon, S.B., Bingham, R. and Mills, D.J. (2017) 'Advances in corrosion protection by organic coatings: What we know and what we would like to know', Progress in Organic Coatings, 102, pp. 2–7. doi: 10.1016/j.porgcoat.2016.04.030.

[5] Funke, W. (1997) 'Problems and progress in Organic Coatings Science and Technology', Progress in Organic Coatings, 31(1–2), pp. 5–9. doi: 10.1016/s0300-9440(97)00013-1.

[6] Vega, J.M. *et al.* (2017) 'Exploring the corrosion inhibition of aluminium by coatings formulated with Calcium Exchange bentonite', *Progress in Organic Coatings*, 111, pp. 273–282. doi:10.1016/j.porgcoat.2017.04.046.

[7] Du, Z. *et al.* (2016) 'The review of Powder Coatings', *Journal of Materials Science and Chemical Engineering*, 04(03), pp. 54–59. doi:10.4236/msce.2016.43007.

[8] Misev, T.A. and van der Linde, R. (1998) 'Powder coatings technology: New developments at the turn of the century', *Progress in Organic Coatings*, 34(1–4), pp. 160–168. doi:10.1016/s0300-9440(98)00029-0.

[9] Czachor-Jadacka, D., Biller, K. and Pilch-Pitera, B. (2023) 'Recent development advances in bio-based powder coatings: A Review', *Journal of Coatings Technology and Research*, 21(2), pp. 435–444. doi:10.1007/s11998-023-00849-5.

[10] Fernández-Álvarez, M. *et al.* (2024) 'Weathering effect on the wear performance of epoxy powder coatings reinforced with calcium ion-exchanged amorphous silica', *Progress in Organic Coatings*, 197, p. 108837. doi:10.1016/j.porgcoat.2024.108837.

[11] Fernández-Álvarez, M., Velasco, F., Bautista, A., Gonzalez-Garcia, Y., *et al.* (2020) 'Corrosion protection in chloride environments of nanosilica containing epoxy powder coatings with defects', *Journal of The Electrochemical Society*, 167(16), p. 161507. doi:10.1149/1945-7111/abd003.

[12] Fernández-Álvarez, M., Velasco, F., Bautista, A. and Abenojar, J. (2020) 'Effect of silica nanoparticles on the curing kinetics and erosion wear of an epoxy powder coating', *Journal of Materials Research and Technology*, 9(1), pp. 455–464. doi:10.1016/j.jmrt.2019.10.073.

[13] Fernández-Álvarez, Maria *et al.* (2020) 'Manufacturing and characterization of coatings from Polyamide powders functionalized with nanosilica', *Polymers*, 12(10), p. 2298. doi:10.3390/polym12102298.

[14] Fernández-Álvarez, M., Velasco, F. and Bautista, A. (2018) 'Effect on wear resistance of nanoparticles addition to a powder polyester coating through ball milling', *Journal of Coatings Technology and Research*, 15(4), pp. 771–779. doi:10.1007/s11998-018-0106-z.

[15] Pilch-Pitera, B. *et al.* (2016) 'Structure and properties of polyurethane-based powder clear coatings systems modified with hydrotalcites', *Progress in Organic Coatings*, 95, pp. 120–126. doi:10.1016/j.porgcoat.2016.03.009.

[16] Vega, J.M. *et al.* (2017a) 'Exploring the corrosion inhibition of aluminium by coatings formulated with Calcium Exchange bentonite', *Progress in Organic Coatings*, 111, pp. 273–282. doi:10.1016/j.porgcoat.2017.04.046.

[17] Liu, Z. *et al.* (2016) 'Experimental investigation on liquid distribution of filter cartridge during gas-liquid filtration', *Separation and Purification Technology*, 170, pp. 146–154. doi:10.1016/j.seppur.2016.06.032.

[18] Jones, R.R. *et al.* (2019) 'Raman techniques: Fundamentals and frontiers', *Nanoscale Research Letters*, 14(1). doi:10.1186/s11671-019-3039-2.

[19] McCreery, R.L. (2005) *Raman spectroscopy for chemical analysis*. Hoboken: John Wiley & Sons.

[20] Fernández-Álvarez, M. *et al.* (2025) 'Raman spectroscopy study of the role of dispersion and interfaces in the improvement of the mechanical properties of epoxy-TiO_2 composites', *Journal of Materials Research and Technology*, 34, pp. 1744–1758. doi:10.1016/j.jmrt.2024.12.181.

[21] Abiko, K. *et al.* (2019) 'Raman imaging of residual stress distribution in epoxy resin and metal interface', *Journal of Raman Spectroscopy*, 51(1), pp. 193–200. doi:10.1002/jrs.5756.

[22] Jansomboon, W. *et al.* (2020) 'Raman spectroscopic study of reinforcement mechanisms of electron beam radiation crosslinking of natural rubber composites filled with graphene and silica/graphene mixture prepared by latex mixing', *Composites Part C: Open Access*, 3, p. 100049. doi:10.1016/j.jcomc.2020.100049.

[23] Zhang, Z. *et al.* (2020) 'Synthesis of a novel dual layered double hydroxide hybrid nanomaterial and its application in epoxy nanocomposites', *Chemical Engineering Journal*, 381, p. 122777. doi:10.1016/j.cej.2019.122777.

[24] Menczel, Menczel, J.D. and Prime, R.B. (2014) *Thermal analysis of polymers: Fundamentals and applications*. Somerset: Wiley.

[25] Khruschov, M.M. (1974) 'Principles of abrasive wear', *Wear*, 28(1), pp. 69–88. doi:10.1016/0043-1648(74)90102-1.

[26] Musil, J. *et al.* (2002) 'Relationships between hardness, Young's modulus and elastic recovery in hard nanocomposite coatings', *Surface and Coatings Technology*, 154(2–3), pp. 304–313. doi:10.1016/s0257-8972(01)01714-5.

[27] Korsunsky, A.M. *et al.* (1998) 'On the hardness of coated systems', *Surface and Coatings Technology*, 99(1–2), pp. 171–183. doi:10.1016/s0257-8972(97)00522-7.

[28] Li, J. *et al.* (2021) 'Thermomechanical properties of epoxy resin/basalt fiber/hydrotalcite composites and influence of hydrotalcite particle size on their properties', *Polymer Composites*, 43(2), pp. 955–963. doi:10.1002/pc.26425.

[29] Aminifazl, A., Karunarathne, D.J. and Golden, T.D. (2024) 'Synthesis of silane functionalized LDH-modified nanopowders to improve compatibility and enhance corrosion protection for epoxy coatings', *Molecules*, 29(4), p. 819. doi:10.3390/molecules29040819.

[30] Mat Yazik, M.H. *et al.* (2021) 'Effect of nanofiller content on dynamic mechanical and thermal properties of multi-walled carbon nanotube and Montmorillonite Nanoclay Filler hybrid shape memory epoxy composites', *Polymers*, 13(5), p. 700. doi:10.3390/polym13050700.

[31] Hernandez, M. *et al.* (2014) 'Characterization of the protective properties of hydrotalcite on hybrid organic-inorganic sol-gel coatings', *Corrosion*, 70(8), pp. 828–841. doi:10.5006/0909.

[32] Marghalani, H.Y. (2010) 'Effect of filler particles on surface roughness of experimental composite series', *Journal of Applied Oral Science*, 18(1), pp. 59–67. doi:10.1590/s1678-77572010000100011.

[33] Karami, Z. et al. (2020) 'Exploring curing potential of epoxy nanocomposites containing nitrate anion intercalated mg–al–LDH with cure index', Progress in Organic Coatings, 139, p. 105255. doi:10.1016/j.porgcoat.2019.105255.

[34] Fernández-Álvarez, M. *et al.* (2021) 'Hindering the decrease in wear resistance of UV-exposed epoxy powder coatings by adding nano-sio2 through ball milling', *Wear*, 480–481, p. 203935. doi:10.1016/j.wear.2021.203935.

[35] Miletić, A. *et al.* (2021) 'Nanolayer CrAlN/Tisin coating designed for tribological applications', *Ceramics International*, 47(2), pp. 2022–2033. doi:10.1016/j.ceramint.2020.09.034.

[36] Chen, Y.-H., Huang, E. and Yu, S.-C. (2009) 'High-pressure Raman study on the series', *Solid State Communications*, 149(45–46), pp. 2050–2052. doi: 10.1016/j.ssc.2009.08.023.